

Modelling and Design of Circularly Masked Two-Dimensional Antenna Arrays

Yasser A. Albagory

Department of Electronics and Communications Engineering, Faculty of Electronic Engineering, Menoufia University,
Menouf, Egypt

College of Computers and Information Technology, Taif University, Saudi Arabia

Abstract: In this paper, the masked two-dimensional array is modelled and designed to reduce the sidelobe levels at no extra processing or optimization for the elements locations and feedings. The masking will turn off the elements at the four corners with a circular boundary function and results in a redistribution and reduction of the sidelobes at the cost of increasing other negligible sidelobes. The new masked two-dimensional array has the advantage of easy manufacturing compared with the concentric circular arrays while maintaining almost the same sidelobe levels and patterns. The analysis of the proposed masked array shows that the sidelobe levels will be reduced by 4 dB at first sidelobe in the two major sidelobe planes (i.e. $\theta = 0^\circ$ and 90°) and is more reduced by up to 10 dB at other sidelobes. In addition, the sidelobe levels can be further reduced by applying any other sidelobe reduction technique as add-on improvement to the array pattern.

Keywords: Array processing, Two-dimensional arrays, Sidelobe reduction, Beamforming.

I. INTRODUCTION

Antenna arrays have an important role in most of communications systems including radar, sonar, mobile, satellites, and many others. The signals received from the antenna elements can be processed to obtain the desired signal while eliminating other unwanted ones. This property has an important impact on the system performance especially the carrier-to-interference ratio and hence improving system capacity and also the provided services. One of main important parameters of the array is its configuration which affect both of the fabrication and capabilities. One dimensional array can detect signals effectively only in one plane and therefore is used in one-dimensional beamforming applications [1]. Circular array can be used in two-dimensional beamforming and has many applications especially in direction-of-arrival estimation (DOA) but suffers from the high sidelobe level which is approximately 8 dB below the main lobe level [2-3]. Concentric circular array (CCA) is another array configuration where a number of circular arrays with different sizes are co-centered [4-5]. CCA has the capability of beamforming in two-dimensions and provides radiation pattern which is almost independent on the azimuth angle of the array [4]. In addition, the sidelobe level is reduced in the CCA and is approximately 17 dB below the mainlobe level [4]. One major disadvantage of the CCA is the difficulty in fabrication where the separation and location of the elements are aligned circularly. For microstrip antenna arrays, the CCA provides difficulties in the feeding and alignment for each antenna element in the array. Another important and practical antenna array configuration is the two-dimensional planar array where the elements are aligned in a two-dimensional plane with regular antenna locations and separations [3, 6-8]. This last configuration makes it easy to fabricate the array with any antenna type. A

disadvantage of the two-dimensional planar array compared to CCA is the relatively higher sidelobe level which is about 13 dB below the mainlobe level. These higher sidelobe levels are almost aligned in two perpendicular planes with other reduced sidelobes in between. This sidelobes distribution is mainly dependent on the elements at the four corners of the array and can be reduced by controlling the feeding of these elements.

Therefore in this paper, the two-dimensional planar array is designed to reduce the effect of corner elements on the sidelobe levels and distribution. The array will be simply masked with a certain masking matrix to reduce the sidelobe levels at minimum processing requirements to gain almost the same sidelobe level as in CCA while maintain the advantage of easy fabrication of two-dimensional arrays.

The paper consists of seven parts and is arranged as follows; in section II, the beamforming system of masked two-dimensional array is introduced and the masking matrix is formulated in Section III. The circular mask is provided in Section IV and its impact on the array radiation pattern is demonstrated in Section V. Finally, Section VI provides some conclusions for the paper.

II. BEAMFORMER FOR MASKED RECTANGULAR ARRAYS

In this section we will describe a general geometry of rectangular arrays with masking. The geometry is shown in Fig. 1 where a rectangular array resides in the xy -plane and an observation point P is located at a spherical co-ordinate (r, θ, ϕ) . The mask will screen some of selected elements especially at the edges of the array while it can also screen other interior elements according to the required design of the radiation beam.

Assuming equidistant element separation of half-wavelength and isotropic elements with neglected

coupling effects, we can write a general steering matrix for the uniform planer array as follows:

$$S_{M,N}(\theta, \phi) = (s_{M,1}(\theta, \phi), s_{M,2}(\theta, \phi), \dots, s_{M,n}(\theta, \phi), \dots, s_{M,N}(\theta, \phi)) \quad (1)$$

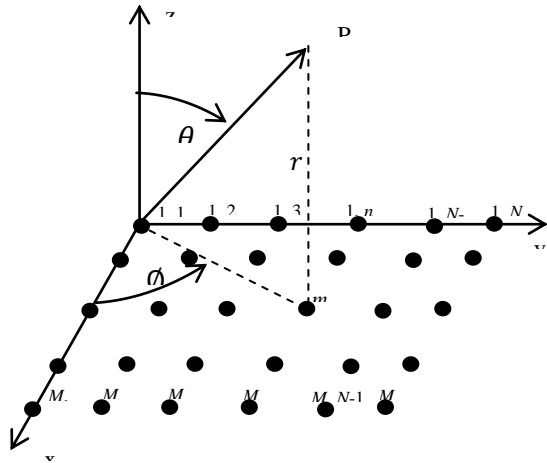


Fig. 1 Antenna elements arrangement in two-dimensional array

where $s_{M,n}(\theta, \phi)$ is the one-dimensional array steering vector of the n th array in the y -direction having M elements and is given by:

$$s_{M,n}(\theta, \phi) = \begin{pmatrix} e^{j2\pi R_{1,n} \sin(\theta) \cos(\phi_{1,n})} \\ e^{j2\pi R_{2,n} \sin(\theta) \cos(\phi_{2,n})} \\ \vdots \\ e^{j2\pi R_{m,n} \sin(\theta) \cos(\phi_{m,n})} \\ \vdots \\ e^{j2\pi R_{M,n} \sin(\theta) \cos(\phi_{M,n})} \end{pmatrix} \quad (2)$$

where $R_{m,n}$ is the normalized distance from the element (m, n) to the origin of the coordinates and is given by:

$$R_{m,n} = \frac{1}{2} \sqrt{(m-1)^2 + (n-1)^2} \quad (3)$$

and $\phi_{m,n}$ is given by:

$$\phi_{m,n} = \phi - \tan^{-1} \left(\frac{m-1}{n-1} \right) \quad (4)$$

The beamformer for masked rectangular arrays is depicted in Fig. 2 where the weighting matrix of the array is comprised by two parts: the first is the mask prescreening matrix and the second is a general add-on weighting matrix and may be for example a tapered function for further sidelobe reduction.

III. GENERAL FORMULATION OF THE MASKING MATRIX FOR RECTANGULAR ARRAYS

The masking matrix is simply a rectangular matrix of the same size as the steering matrix $S_{M,N}(\theta, \phi)$ or of $M \times N$ elements and each element in this matrix is equal to either 1 or 0 according to the screening figure applied to the

array. The zeros in the mask matrix are simply representing permutation of the corresponding antenna elements.

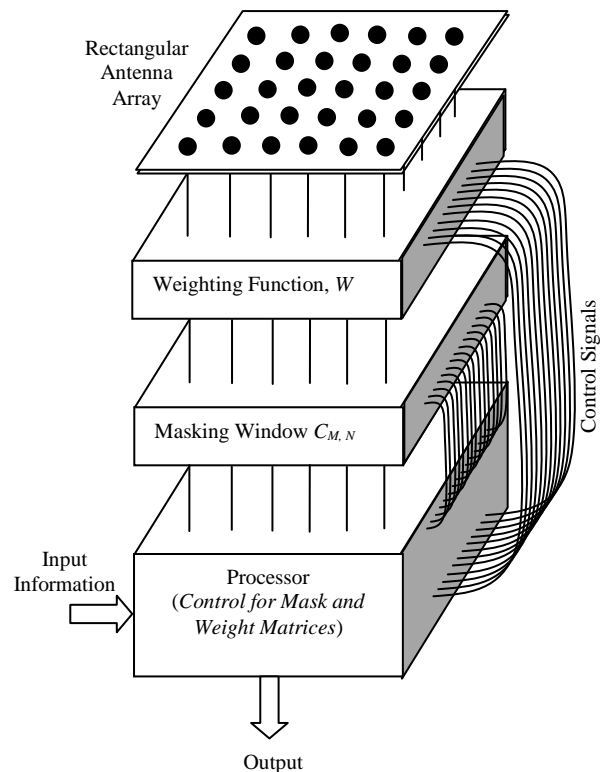


Fig. 2: Beamformer for masked two-dimensional array Denoting the masking matrix as $C_{M,N}$ and the mn^{th} element in this matrix as $c_{m,n}$, therefore we can write an expression for the mn^{th} element in the masked steering matrix, $S_{M,N} * C_{M,N}$, as $c_{m,n} s_{m,n}$ where $s_{m,n}$ is the m^{th} element in the n^{th} steering vector and the operator $*$ represents an element multiplication

Therefore the masked matrix, $S_{M,N} * C_{M,N}$ is formed as follows:

$$S_{M,N} * C_{M,N} = \begin{pmatrix} c_{1,1} s_{1,1} & c_{1,2} s_{1,2} & \dots & c_{1,n} s_{1,n} & \dots & c_{1,N} s_{1,N} \\ c_{1,1} s_{2,1} & c_{1,2} s_{2,2} & \dots & c_{1,n} s_{2,n} & \dots & c_{1,N} s_{2,N} \\ \vdots & \vdots & \ddots & \vdots & \ddots & \vdots \\ c_{m,1} s_{m,1} & c_{m,2} s_{m,2} & \dots & c_{m,n} s_{m,n} & \dots & c_{m,N} s_{m,N} \\ \vdots & \vdots & \ddots & \vdots & \ddots & \vdots \\ c_{M,1} s_{M,1} & c_{M,2} s_{M,2} & \dots & c_{M,n} s_{M,n} & \dots & c_{M,N} s_{M,N} \end{pmatrix} \quad (6)$$

Figure 2 displays a mapped array to cope with the masked steering matrix where the x -axis is directed downward while the y -axis is towards the right hand.

There are several possible shapes of the array mask according to the shape of the array edges. Figure 4 displays a set of possible masking matrix including triangular-cut edges, rounded edges, hole-plus-edges, and nonuniform edges. The masking matrix can be also shaped in its interior only or in both interior and at the edges.

These varieties in shaping rectangular arrays open more opportunities for the beam design to suit the required shape. In the next section, we will examine some of these masks and demonstrate how to formulate the corresponding matrix, show the overall weighting matrix of the shaped array, and depict the effect of masking on the radiation pattern, beam shape and sidelobe levels.

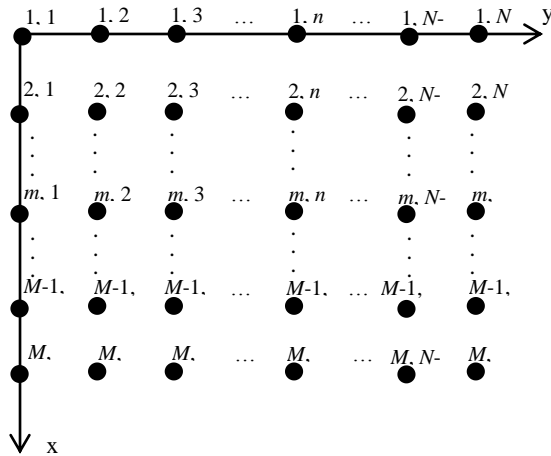


Fig. 3 Elements arranged in a matrix for the formulation of the masking matrix

IV. MASKING MATRIX FOR CIRCULAR EDGES TWO DIMENSIONAL ARRAYS

In this section, the masking matrix will be formulated for the circular rounded rectangular array edges. Assume that the array is formed and arranged as shown in Fig. 3 by matrix of $M \times N$ isotropic elements. Generally, the value of M and N may be different in value therefore we will divide the overall array matrix into five sub matrices as shown in Fig. 5 where four of them are located at the array edges while the remaining fifth sub matrix is located at the middle of the array and is oriented either vertically or horizontally according to whether M or N is greater. In Fig. 5, it is assumed that $M > N$ so there will be a stripe of elements in the horizontal direction around the array middle.

We will formulate the mask sub matrix at the first upward left side of the array (Q_1), then extending the definition to include the overall masking matrix. As $M \geq N$, then the dimension of the first corner matrix will be given by:

$$length(Q_1) = \begin{cases} \frac{N}{2} & \text{for } N \text{ even} \\ \frac{N+1}{2} & \text{for } N \text{ odd} \end{cases} \quad (7)$$

If $N > M$, then (7) will be

$$length(Q_1) = \begin{cases} \frac{M}{2} & \text{for } M \text{ even} \\ \frac{M+1}{2} & \text{for } M \text{ odd} \end{cases} \quad (8)$$

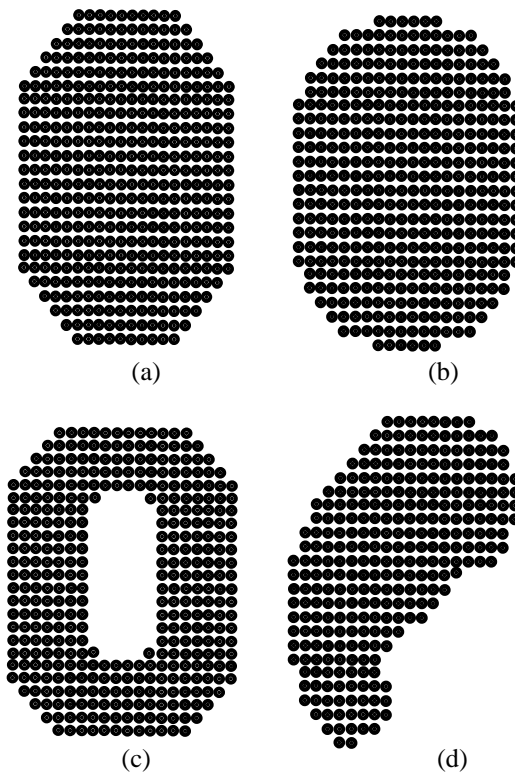


Fig. 4 Typical mask patterns for the two-dimensional array

The masking procedure for almost-rounded circular edges will be obtained by quantization process for the excluded or masked elements. This process performs the following steps:

- 1- Convert the element index into a radial index distance from the downward right corner point in the sub array matrix.
- 2- Compare this distance for each element in this sub matrix to a threshold radial distance.
- 3- Exclude elements greater than this threshold.

The radial index radius is measured from the last element in the sub matrix to any element within this matrix. The last element in the corner sub matrix is denoted by the local origin index or (I_{Qi}) where i is the index of the quarter.

The origin index of the first corner sub matrix is located at:

$$I_{Q1} = \begin{cases} \left(\frac{N}{2}, \frac{N}{2}\right) & \text{for } M \geq N \text{ and } N \text{ is even} \\ \left(\frac{N+1}{2}, \frac{N+1}{2}\right) & \text{for } M \geq N \text{ and } N \text{ is odd} \\ \left(\frac{M}{2}, \frac{M}{2}\right) & \text{for } N > M \text{ and } M \text{ is even} \\ \left(\frac{M+1}{2}, \frac{M+1}{2}\right) & \text{for } N > M \text{ and } M \text{ is odd} \end{cases} \quad (9)$$

The first corner radial index distance from any element of indices (m, n) in this quarter (i.e. $m = 1, 2, 3, \dots, M/2$ and $n = 1, 2, 3, \dots, N/2$) and to the local origin index of that quarter is given by:

$$d_{Q1}(m, n) = \begin{cases} \sqrt{\left(\frac{N}{2} - m\right)^2 + \left(\frac{N}{2} - n\right)^2} & M \geq N, N \text{ even} \\ \sqrt{\left(\frac{N+1}{2} - m\right)^2 + \left(\frac{N+1}{2} - n\right)^2} & M \geq N, N \text{ odd} \\ \sqrt{\left(\frac{M}{2} - m\right)^2 + \left(\frac{M}{2} - n\right)^2} & N > M, M \text{ even} \\ \sqrt{\left(\frac{M+1}{2} - m\right)^2 + \left(\frac{M+1}{2} - n\right)^2} & N > M, M \text{ odd} \end{cases} \quad (10)$$

The threshold index distance (T_{Q1}) for the circular edge array will range from a minimum value corresponding to the indices:

$$T_{Q1min} = \begin{cases} \frac{N}{2} - 1 & M \geq N, N \text{ even or even} \\ \frac{M}{2} - 1 & N > M, M \text{ even or even} \end{cases} \quad (11)$$

And the maximum will be at $(1, 1)$ or

$$T_{Q1max} = \begin{cases} \sqrt{2} \left(\frac{N}{2} - 1\right) & M \geq N, N \text{ even} \\ \sqrt{2} \left(\frac{N+1}{2} - 1\right) & M \geq N, N \text{ odd} \\ \sqrt{2} \left(\frac{M}{2} - 1\right) & N > M, M \text{ even} \\ \sqrt{2} \left(\frac{M+1}{2} - 1\right) & N > M, M \text{ odd} \end{cases} \quad (12)$$

Therefore we may write T_{Q1} as follows:

$$T_{Q1min} \leq T_{Q1} \leq T_{Q1max} \quad (13)$$

Noting that in the case of maximum threshold value, the array will be not masked and all antenna elements will participate in the overall gain of the array.

Now the masking matrix in the first quarter will realize the following criteria:

$$C_{M,N|Q1} = \begin{cases} 1 & \text{if } d_{Q1}(m, n) \leq T_{Q1} \\ 0 & \text{if } d_{Q1}(m, n) > T_{Q1} \end{cases} \quad (14)$$

Figure 5 shows the variation of the radial index distance with the element indices in the upper-left quarter and assuming square even array (i.e. $M = N$ and M and N are even and equal 40).

Actually the masking procedure performs digital masking for the array elements at the corners where the elements with index distance greater than the threshold value will be trimmed. The profile of the new edges is not necessarily circular due to the elements distribution but at lower threshold distances near the minimum value, it will be almost rounded in a circular way.

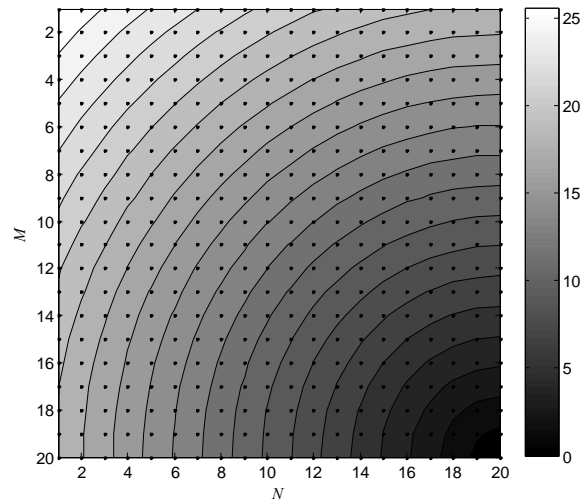


Fig. 5 Antenna elements arrangement and radial index distance profile

Now, the second corner sub mask matrix can be easily found as follows:

$$C_{M,N|Q2} = FlipHoriz(C_{M,N|Q1}) \quad (15)$$

while the third corner sub masking matrix can will be:

$$C_{M,N|Q3} = FlipVert(C_{M,N|Q1}) \quad (16)$$

and finally, the fourth corner sub masking matrix can will be:

$$C_{M,N|Q4} = FlipVert(C_{M,N|Q2}) \quad (17)$$

where the operator *FlipVert* rotates the matrix by 180° vertically while *FlipHori* rotates the matrix by 180° horizontally.

In the case where $M \neq N$, there will be a “stripe” sub matrix which is located at the middle of the array either vertically or horizontally. This sub matrix has the dimensions of $M - N \times N$ if $M \geq N$ or $N - M \times M$ if $N > M$ and is formed by ones (1) inserted into the overall masking matrix to have the same size of the array.

Therefore the overall masking matrix will be given by:

$$C_{M,N} = \begin{cases} \begin{pmatrix} C_{M,N|Q1} & C_{M,N|Q2} \\ \mathbf{1} & \mathbf{1} \\ C_{M,N|Q3} & C_{M,N|Q4} \end{pmatrix} & M \geq N \\ \begin{pmatrix} C_{M,N|Q1} & \mathbf{1} & C_{M,N|Q2} \\ C_{M,N|Q3} & \mathbf{1} & C_{M,N|Q4} \end{pmatrix} & N > M \end{cases} \quad (18)$$

This matrix may be further rotated by any angle according to the azimuth direction of the beam.

V. PERFORMANCE OF CIRCULARLY MASKED-RECTANGULAR ARRAYS

Now we will examine the radiation characteristics of the rectangular masked arrays where the masking operation will be performed at the corners of the array. Assume an array of 40×40 elements. The beam will be formed

towards the array broadside direction (i.e. $(\theta, \phi) = (0,0)$). As shown in Fig. 6, the array is masked at the edges by different normalized threshold values (1, 0.9, 0.8, and 0.707). The normalized threshold ($T_{Q1|N}$) is given by:

$$T_{Q1|N} = T_{Q1}/T_{Q1max} \quad (19)$$

As the normalized threshold decreases, more elements are excluded from the array at the corners and the array has almost circular edges at $T_{Q1|N} = 0.707$. The effect of the masking operation at different normalized thresholds is depicted in Fig. 7 where the array normalized gain is displayed at different planes of ϕ for the same arrays in Fig. 6 respectively. In general, the rounded masks in Fig. 6 will redistribute the sidelobes of the array in both angles and levels. In Fig. 7(a), there is no masking and there will be two major planes at which the highest sidelobes are located. These planes are at $\phi = 0^\circ$ and $\phi = 90^\circ$. Reducing the threshold slightly will reduce slightly the main sidelobes levels and the raise the other lower sidelobes.

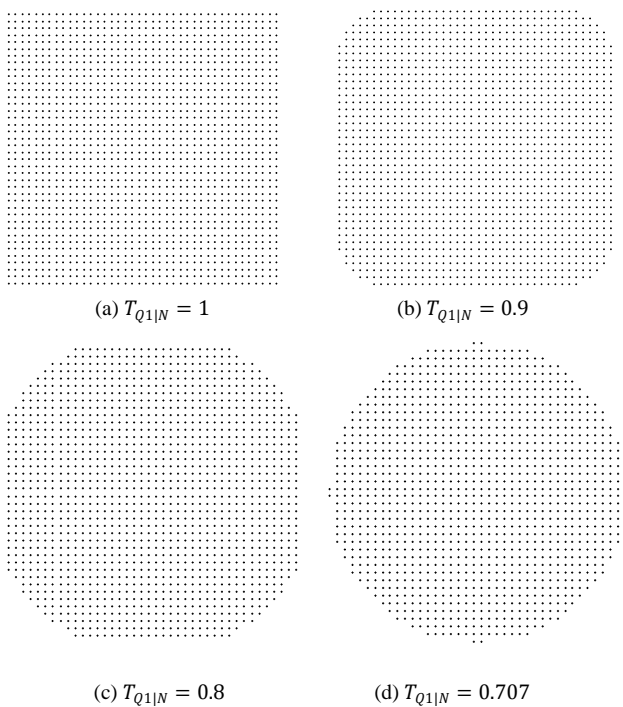


Fig. 6 Masked array at different values of the normalized threshold

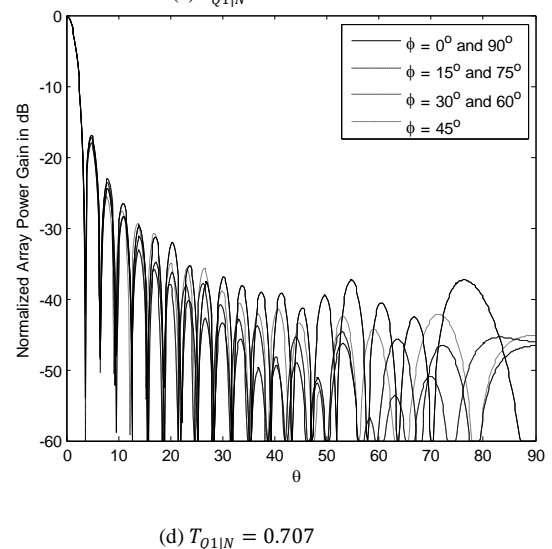
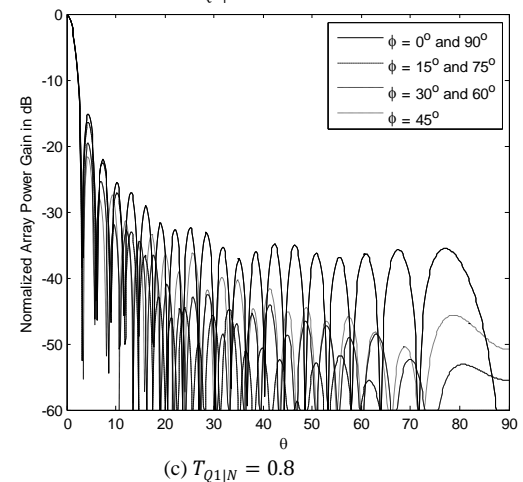
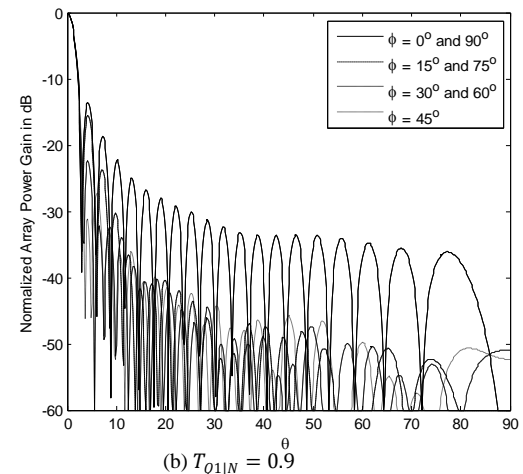
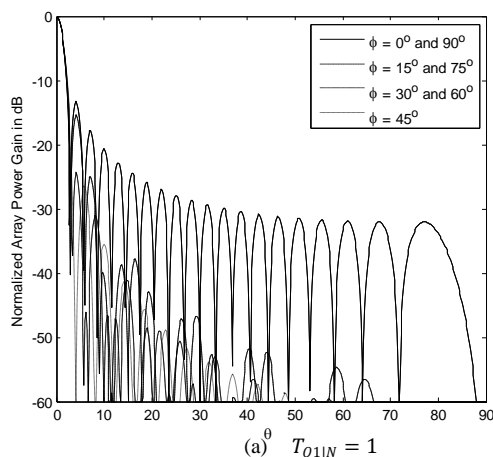


Fig. 7 Normalized array power patterns at different values of the normalized threshold

The process continues as in Fig. 7(c) where the sidelobe levels at $\phi = 0^\circ$ and $\phi = 90^\circ$ are reduced while the other planes of ϕ will raise and finally at $T_{Q1|N} = 0.707$, almost sidelobes have equal envelopes as shown in Fig. 7(d) but the highest envelope will be lower than that in Fig. 7(a) by at least 3dB at the first sidelobe.

Figure 8 demonstrates the effect of masking on the major sidelobe planes (i.e. at $\phi = 0^\circ$ and $\phi = 90^\circ$) for $T_{Q1|N} = 1$

and $T_{Q1|N} = 0.707$ where the major sidelobes envelopes has reduced by 3 dB at the first sidelobe and are down by approximately 10 dB near the endfire direction of the array. This reduction in sidelobe levels has been actually done without performing any processing for the array weights. The mainlobe can be directed by simply adjusting only the phases of the signals at the array elements as in conventional phased arrays.

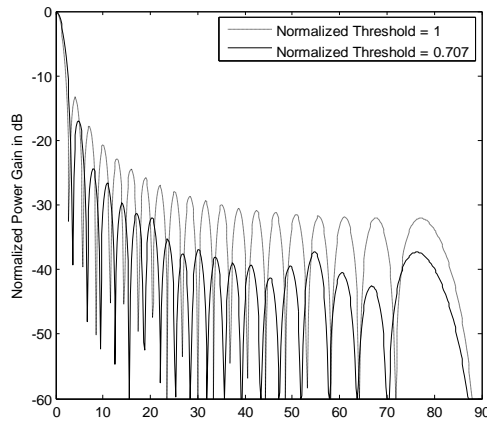
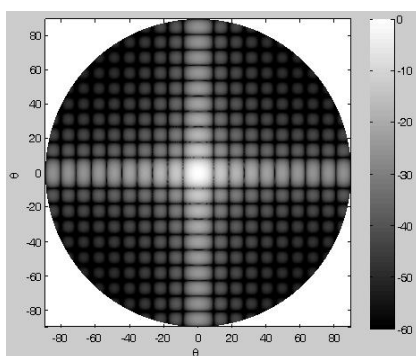
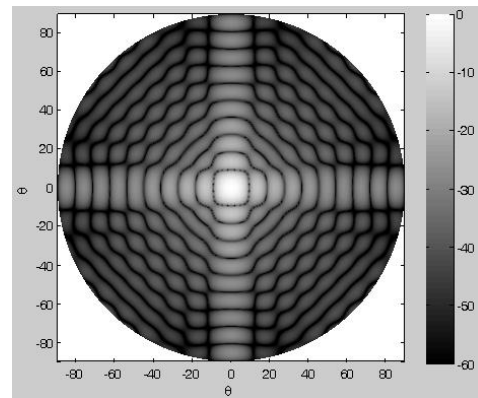


Fig. 8 The normalized power pattern of the array at $T_{Q1|N} = 1$ and 0.707 for the major sidelobe plane at $\theta = 0$ and 90 degrees

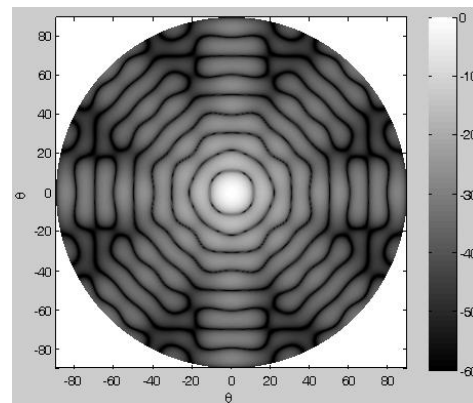
A complete view for the array radiation pattern at different values of $T_{Q1|N}$ is shown in Fig. 9 (a), (b), and (c) where the array size is 20×20 elements. In these figures, the isolated spots represent sidelobes in the pattern. These isolated spots will merge and dissolve together and are converted to almost ring sidelobes as shown in Fig. 9 (c) at $T_{Q1|N} = 0.707$. An important notice in these figures is that the masking operation will reduce the number of elements of the array and correspondingly the array gain will be reduced also, therefore for proper comparison we should compensate the masked array with extra elements by pre-incrementing the array size at $T_{Q1|N} = 1$ so that after masking the number of elements will be almost the same. For example, the total number of elements at an array size of 20×20 is 400 elements which will be reduced to 284 elements and the mainlobe power gain will be reduced by 0.71. Now if we pre-increment the array to 23×23 , this will give 416 elements after masking which is the nearest array size to the original 400 elements. This presetting will compensate for the increased beamwidth as well as the reduced mainlobe gain resulted from the masking operation.



(a) $T_{Q1|N} = 1$ $N = 20$, $M = 20$



(b) $T_{Q1|N} = 0.9$ $N = 20$, $M = 20$



(c) $T_{Q1|N} = 0.707$ $N = 20$, $M = 20$

Fig. 9 Normalized radiation pattern of an array of 20×20 elements at different normalized threshold values. The vertical bar represents the normalized power in dB.

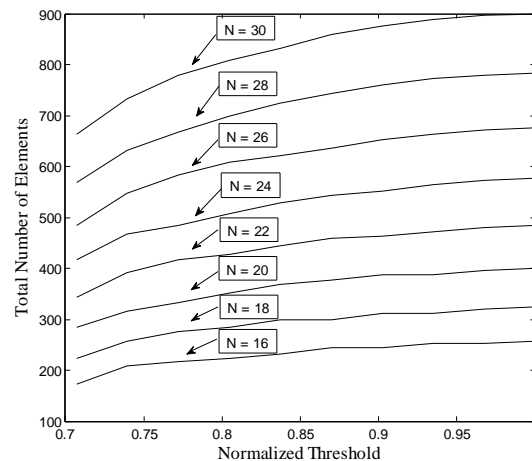


Fig. 10 Variation of the number of elements of a square two-dimensional array with the normalized threshold

Figure 10 shows the reduction in the number of elements at different normalized threshold values and initial sizes. The threshold operation will result in a “quantized” array size because the element corner distance is also a discrete value. That is why we search for the nearest pre-array size. In Fig. 11, the array size variation of square arrays with the one-dimensional number of elements for the unmasked and masked array cases is depicted where in the unmasked array it is simply following quadratic equation while in the

masked array (i.e. $T_{Q1/N} = 0.707$), there will be some minor difference because of the quantization action in the thresholding process. The array size will be almost reduced by the normalized threshold value. As shown in Fig. 12, an approximation for the quantized masked array size at $T_{Q1/N} = 0.707$ is approximated by a quadratic equation with one term and a coefficient equals 0.73. This coefficient is chosen to give negligible difference at the middle range of N and can be moved to lower or higher values which almost lie between 0.71 and 0.74 for the range of N is 18 to 40 elements.

Therefore a rough approximation of the ore-array size is given by:

$$N_{pre} = \left\lfloor \frac{1}{\sqrt{\sigma}} N \right\rfloor_{T_{Q1/N}=0.707} \quad (20)$$

where σ is given by:

$$0.71 \leq \sigma \leq 0.74 \quad (21)$$

and the operator $\lfloor \cdot \rfloor$ represents the nearest lower integer to the original unmasked array size. The value of σ is chosen so that the interception between the two curves occurs at the desired N . For example, if $N = 30$ we may choose $\sigma = 0.73$ while at $N = 40$, the value of $\sigma = 0.74$. The lowest value of $\sigma = 0.71$ is chosen at $N = 18$ elements.

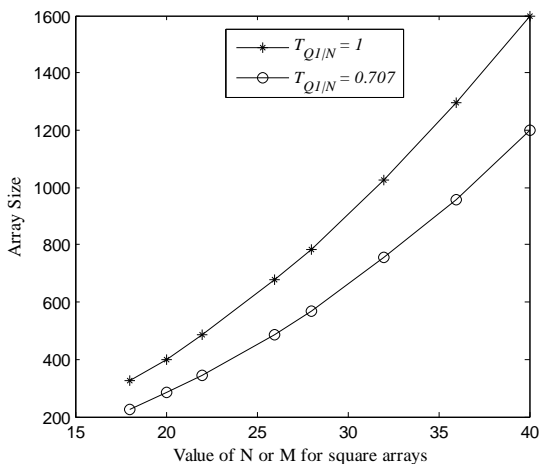


Fig. 11 Array size versus the initial number of elements for the unmasked square array and full circle masked array.

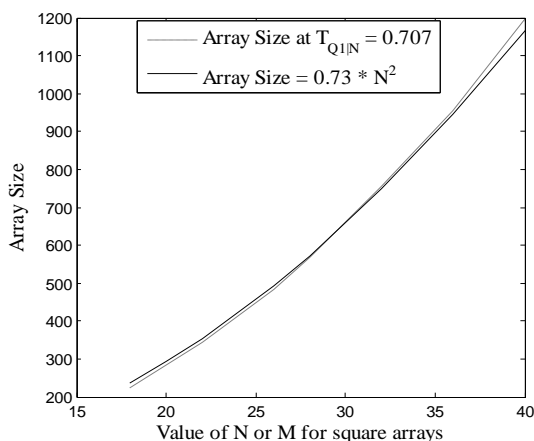


Fig. 12 Variation of the array size with the initial number of elements at $T_{Q1/N} = 0.707$ and an approximately equivalent relation for the same array.

Fig. 13 depicts the radiation patterns of almost the same number of elements while one is unmasked and the other is masked at $T_{Q1/N} = 0.707$. The two arrays almost have the same beamwidth and the unmasked array has a size of 18×18 elements (i.e. total of 324 elements) while the other array is designed by 22×22 pre-incremented masked array and the actual total number of elements is 344 elements. After designing the masked array, the active elements are only implemented and practically fabricated. There will be a negligible difference between the two array power gains due to the extra 20 elements in the masked array and the percentage of power gain increase is only 0.38%.

The two major sidelobe planes are shown in Fig. 13 where by using almost the same number of elements, the masked array will have reduced sidelobe levels starting from approximately 3 dB decrease for the first sidelobe level (i.e. -17 dB for the masked array) to more than 10 dB at some other sidelobes.

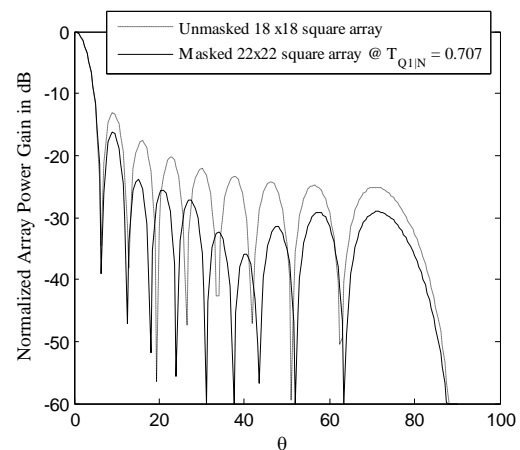


Fig. 13 Sidelobe reduction due to masking for almost equal size arrays.

VI. CONCLUSION

In this paper, the two-dimensional array has been designed with a lower sidelobe level without any extra processing by masking the elements at the corners of the array. The analysis of this array has shown that an array can be designed by almost the same number of elements with rounded array corners and provide more than 4 dB reduction in the sidelobe level and can be 10 dB at farther sidelobes. The New design has the advantage of the simple two-dimensional array manufacturing compared to the concentric circular array which gives the same sidelobe level.

REFERENCES

- [1] L. Godara, "Application of antenna arrays to mobile communications, Part II: beam-forming and direction of arrival considerations", *Proceeding of IEEE*, Vol. 85, No. 8, pp. 1195-1245, Aug. 1997.
- [2] Bogdan L. Comsa C. "Analysis of circular arrays as smart antennas for cellular networks". *Proc IEEE int symp signals circuits and systems '03*, vol. 2, July. 2003. p. 525-8.
- [3] Balanis CA. "Antenna theory: analysis and design", New York: Harper Row; 1982.

- [4] Moawad Dessouky, Hamdy Sharshar, Yasser Albagory, "Efficient Sidelobe Reduction Technique for Small-Sized Concentric Circular Arrays", *Progress In Electromagnetics Research*, PIER 65, pp. 187-200, 2006.
- [5] Mostafa Nofal, Sultan Aljahdali and Yasser Albagory, "Tapered Beamforming for Concentric Ring Arrays", *AEU International Journal of Electronics and Communications*, Vol. 67, No. 1, pp. 58-63, 2013.
- [6] W. Li, X. Huang, and H. Leung "Performance evaluation of digital beamforming strategies from satellites", *IEEE Transactions on Aerospace and Electronic Systems*, Vol. 40, No. 1, January 2004.
- [7] Lennin E. Amador, Roberto Conte, David H. Covarrubias "Performance evaluation of planar antenna arrays onboard low earth orbit satellites" *AEU - International Journal of Electronics and Communications*, Volume 64, Issue 4, April 2010, Pages 377–382.
- [8] Lahcene Hadj Abderrahmane, Belgacem Boussoar1, "New optimisation algorithm for planar antenna array synthesis", *AEU - International Journal of Electronics and Communications*, Volume 66, Issue 9, September 2012, Pages 752–757
- [1] J. Padhye, V. Firoiu, and D. Towsley, "A stochastic model of TCP Reno congestion avoidance and control," Univ. of Massachusetts, Amherst, MA, CMPSCI Tech. Rep. 99-02, 1999.
- [2] Wireless LAN Medium Access Control (MAC) and Physical Layer (PHY) Specification, IEEE Std. 802.11, 1997.

BIOGRAPHIES



B.Sc in Electronic Engineering in 1998 and M.Sc in adaptive arrays for mobile radio communications in 2002 from the Faculty of Electronic Eng., Egypt. He also has been awarded the Ph.D degree in Communications Engineering in the field of High-Altitude Platform Wireless

Communications System in 2008. He is a lecturer in the Electronics and Electrical Communications Engineering Department, Faculty of Electronic Engineering, Menoufia University, Egypt. The research interests include adaptive antenna arrays, mobile communications, and high altitude platforms, satellite communications. He is a reviewer of many international conferences and journals in the field of wireless communications and has many journal papers in the area of smart antennas and high-altitude platforms.